Supercapacitor-Buffered DC-Operable Refrigerators for DC Homes

Nirashi Polwaththa Gallage[1], Don Charles Themiya Sirimanne[1], Nihal Kularatna[1], Alistair Steyn-Ross[1],
Dulsha Kularatna-Abeywardana[2],
[1]School of Engineering
University of Waikato, Hamilton 3240, New Zealand
Email:np138@students.waikato.ac.nz, ds399@students.waikato.ac.nz, nihal.kularatna@waikato.ac.nz, asr@waikato.ac.nz
[2]Department of Electrical, Computer and Software
University of Auckland,Auckland 1010, New Zealand
Email: d.abeywardana@auckland.ac.nz

***Abstract*—Efficiency improvements in whiteware will help reduce the overall power consumption of a household. Modern inverter-driven whiteware, such as refrigerators, operates internally on a DC bus, permitting direct powering from the DC bus of a renewable energy system. However, the fluctuating nature of renewable energy DC sources mandates an energy storage system to increase the reliability of DC operations. In this paper, we present the data related to the conversion of a 230 V, 50 Hz AC operable household refrigerator to operate from a solar DC bus, with a supercapacitor bank forming an integral part of a supercapacitor-assisted (SCA) low frequency DC-DC converter. In addition, experimental results of DC camping refrigerator powered from a solar DC bus and the essential details of the new low-frequency SCA converter are also presented.**

***Index Terms*—DC appliances, DC homes, supercapacitors, power converters, renewable energy**

I. Introduction

Energy efficiency of home appliances has always been an important topic in the renewable energy domain. Solar or wind energy-based DC homes and DC microgrids are a new research directions [1–5] to support the efficiency aspects of appliances. Solar energy is fast gaining popularity in harvesting through PV (photovoltaic) arrays as it is distributed throughout the globe; 98% of the world population receives more than 3 kWh/m^2 of solar radiation per day [2]. Since 2008, price of solar PV panels has decreased by 70% and wind turbine costs have decreased by 40%. Significant developments in semiconductor-based converters will lead to price reduction of PV-based DC microgrids in the future [2]. When compared with natural gas-based electricity, US companies are observed that roof-top PV electricity costs were reduced from 36% to 75% during peak hours of the day while initializing solar PV-based DC microgrids [6].

The traditional approach of using solar or wind energy is to use an inverter buffered by a maximum power point tracking (MPPT) based DC-DC converter with or without a battery pack for energy buffering. Currently available solar panels in the market have a maximum efficiency ranging from 20–25% implying that a larger fraction of energy is wasted inside the solar panels during the power transformation stage [6]. Therefore, electrical energy generated by solar PV should be utilized in an effective manner to obtain high end-to-end efficiency (ETEE).

Most state-of-the-art whiteware in the appliance domain is internally powered by a DC bus derived from the 230 V/ 50 Hz or 120 V/ 60 Hz AC source [6–8]. As Fig. 1a depicts, the traditional AC mains supply feeds modern "inverter-driven" whiteware. A first-stage AC-DC converter supplies DC power to the major functional modules such as the brushless DC motor driver. Similarly, in many household appliances and infotainment systems, several cascaded DC-DC converters are used to feed electronic modules, motors, etc. The example illustrated in Fig. 1a with three converter modules has an end-to-end efficiency (ETEE) given by the product of the three individual module efficiencies $\eta = \eta_1\eta_2\eta_3 = 0.86$ for the case $\eta_1 = \eta_2 = \eta_3 = 0.95$. If the same load is supplied by a DC source as in Fig. 1b, the effective ETEE becomes $\eta = \eta_2.\eta_3 = 0.9$, an efficiency improvement of 4% .

However, when an appliance is converted to renewable energy DC operation by removing the AC-DC converter, we face the issue of the fluctuating nature of the DC source; this demands that an energy be stored within the system.

To eliminate environmentally unfriendly batteries and buffer against the DC source fluctuations, our new approach is to utilize supercapacitors (SCs) having long life-cycle to provide an integral part of the power converter for a refrigerator. This paper is organized as follows: Section II describes the operation of the inverter-driven refrigerator in DC operable mode. How to apply the novel concept of adding SC with the inverter-driven refrigerator to enhance efficiency is discussed in Section III. A scaled-down system for proof of concept is presented in Section IV, and Section V describes the conclusion and further work.

II. INVERTER-DRIVEN REFRIGERATOR IN DC OPERABLE MODE

To reduce energy consumption significantly in refrigerators, variable capacity compressors (VCCs) are used with brushless DC (BLDC) motors [9]. Major significance of these refrigerators is the capacity of the compressor is regulated with the load by varying the speed of the motor unless fixed speed running with induction motor in traditional refrigerator. BLDC motors are powered by a three-phase inverter fed by a DC source directly derived from the available AC power line [10, 11]. VCCs provide significant savings of energy of about 30 to 50% [9, 12]. Inverter-driven refrigerators start smoothly at the initial stage without drawing inrush current as high as traditional refrigerators and maintain lower speed that is enough to keep the target temperature in the refrigerator compartment [9, 13]. Fig. 2 shows the current consumption of a commercially available double-door refrigerator (Fisher and Paykel, Model RF402B), based on a test carried out at the laboratory at a room temperature of 20 °C. (Thermostat setting 10 is the coldest and warmest is the setting 1.) The refrigerator draws average current of 0.72 A and 0.3 A at the initial cycle and the steady state cycle respectively.

By removing the front-end AC–DC converter, a direct DC source can be connected to the inverter-driven refrigerator according to the block diagram as shown in Fig. 3.

In such a refrigerator, there are two different DC power rails used to power the BLDC motor by 325 V and the 12 V DC rail for the low energy consuming auxiliary systems. Laboratory measurements identified that this inverter-driven refrigerator operates within the wide range of AC voltage from 180 to 230 V. After removing the AC-DC converter shown in Fig. 3, the operation of the refrigerator was tested for DC operation using a solar simulator capable of DC output up to 600 V at 6.3 A (model TerraSAS). It has been operated over a wide DC voltage range from 255 V DC (related to 180 $\sqrt{2}$V) to 325 V DC (230 $\sqrt{2}$ V) supplied from the solar DC simulator.

Fig. 4 shows the inverter module of the RF 402B refrigerator. AC zone receives the 230 V AC input via its EMC filter and it is connected to the rectifier unit in the DC zone. Rectifier output is fed on to a capacitor of 200 μF rated at 450 V DC creating the DC bus voltage of approx 325 V. The right hand side of the Fig. 4a carries the motor control IC, gate driver IC and the associated low voltage circuitry required by the inverter unit. A 3.3 V DC rail is supplied to this board from the auxiliary control unit of the refrigerator, which is powered separately form a different AC-DC converter. Fig. 4b shows the backside of the same PCB which carries the six transistor switches used for the three-phase inverter.

The auxiliary electronic module carries a processor and associated circuitry for monitoring and controlling the electronic functions such as fans, door sensors, lighting, etc. Fig. 5 depicts this secondary PCB with a separate AC-DC converter. Removing both AC-DC converters and supplying DC from a renewable energy source increases the efficiency while reducing component cost.

Table I provides the power consumption of this inverter-driven refrigerator operating under AC 230 and 180 V as well as DC power conditions created using a 325 V DC bus and a 255 V DC feeds from the solar DC simulator. We clearly see a 5% reduction in power consumption of the DC-modified refrigerator.

TABLE I: Power consumption of the refrigerator for different AC and DC input voltages

	Average power consumption (W)			
Operational voltages (V)	**230 AC**	**325 DC**	**180 AC**	**255 DC**
Initial cycle	102.3	96.4	104.1	98.6
Steady-state cycling	42.7	40.7	41.1	39.2

When an appliance is converted to renewable energy DC operation, we face the issue of the fluctuating nature of the DC source from solar or wind. This demands that an energy storage system be incorporated within the overall system. Our new approach to address this issue is based on the following key ideas:

1) Make use of the wide operational voltage range of a brushless DC (BLDC) motor drive system.

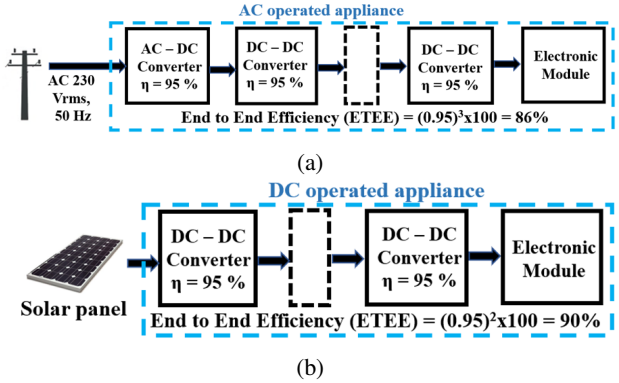

Fig. 1: Appliance internal electrical circuitry running with (a) AC supply; (b) DC supply

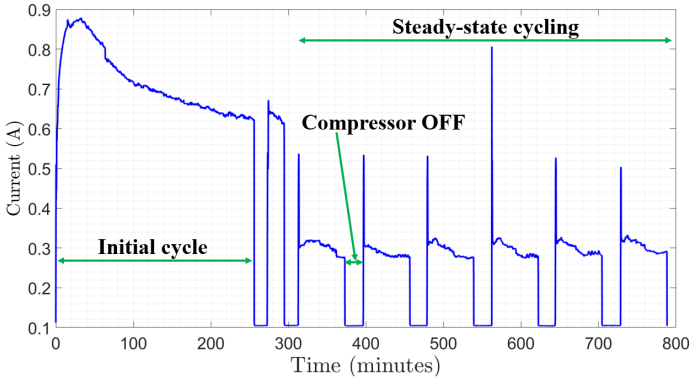

Fig. 2: Current drawn by the inverter-driven refrigerator at 230 V AC in thermostat setting 5.

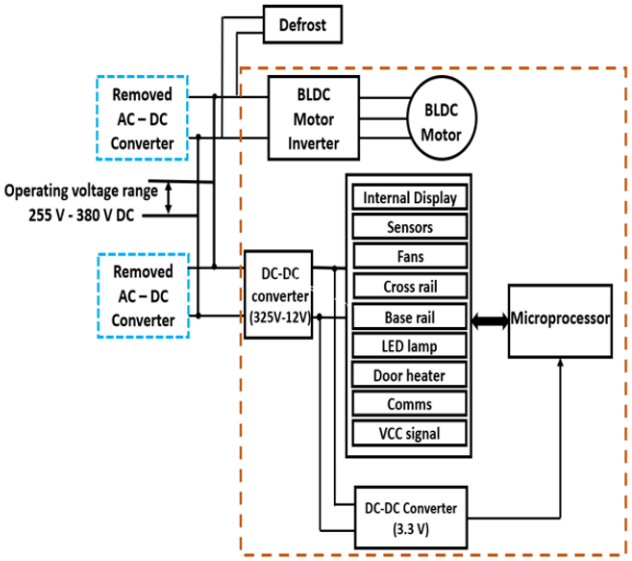

Fig. 3: Block diagram of the typical inverter-driven refrigerator powered from a DC bus based on a renewable source [14].

2) Instead of battery bank, utilize a SC bank having long life-cycle and low electrical series resistance (ESR).

III. POWERING INVERTER- DRIVEN REFRIGERATOR WITH SCs

A. Supercapacitor Assisted Loss Management (SCALoM) concept

This project utilizes the new theoretical concept SCALoM [15] which applied to many supercapacitor assisted (SCA) techniques. SCALoM concept applied to a simple RC circuit which modifies by three specific steps, namely (i) replacing the normal capacitor with a 5 to 7 orders larger capacitor (a SC); (ii) inserting a useful resistive load into loop to usefully-consume the resistive losses in the R-C loop; (iii) Initializing the SC at a non-zero initial voltage.

Referring to Fig. 6a, R_L (effective load resistance) is very large compared to the r_p, parasitic loop resistance and it helps to make parasitic losses much smaller[15–17]. By inserting a SC, we increase the time constant of the circuit by several orders of magnitude. Increasing the cycling time allows the use of low-speed switches with less dynamic switching losses [16, 18, 19]. The low speed switching circuit is designed to ensure charge balance and protect the overcharge of SC.

A SC is connected to the circuit with a pre-charged voltage of kV_W (where V_W is the final capacitor voltage, k is a constant: $0 \leq k \leq 1$), together with the supply voltage increased to $V_S = mV_W$, by a factor of m ($m > 1$) as shown in Fig. 6a. k is defined as the pre-charge factor and m is the power supply over-voltage factor.

According to Fig. 6a,
the energy consumed by the useful load, R_L can be derived as [15, 18];

$$E_{R_L} = \frac{P(1-k)(2m-k-1)V_W^2 C}{2(P+1)} \tag{1}$$

where P is the ratio between R_L and r_p and $P \geq 1$. By keeping the ratio P to be much greater than 1, we shifted the parasitic losses to useful load in typical RC circuit.

The energy dissipated by the parasitic resistance (r_p) of the loop will be:

$$E_{r_p} = \frac{(1-k)(2m-k-1)V_W^2 C}{2(P+1)} \tag{2}$$

The energy stored in the capacitor when it charges from kV_W to V_W can be written as:

$$E_C = \frac{(1-k)V_W^2 C}{2} \tag{3}$$

The total energy supplied by the DC voltage source can be written as from 1, 2 and 3;

$$E_S = E_C + E_{R_L} + E_{r_p} = (1-k)mV_W^2 C \tag{4}$$

The efficiency of the charging loop will be:

$$\eta = \frac{E_C + E_{R_L}}{E_S} = \frac{1}{1+P}\left(P + \frac{1+k}{2m}\right) \tag{5}$$

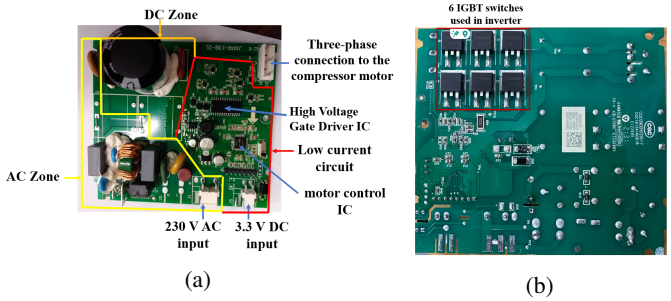

(a) (b)

Fig. 4: Inverter module of the RF402B refrigerator (a) front side; (b) back side

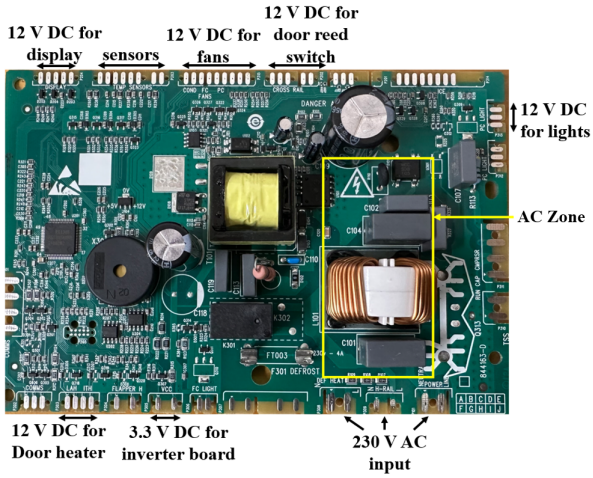

Fig. 5: Auxiliary circuit of the RF402B refrigerator

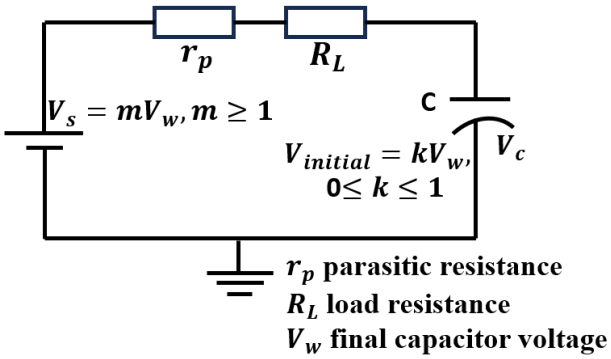

(a)

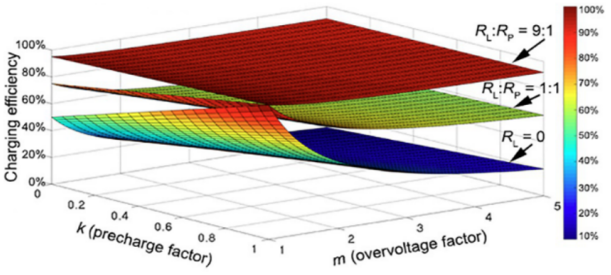

(b)

Fig. 6: Capacitor charging phase (a) capacitor charging circuit with useful load; (b) graphical representation of the circuit behavior in terms of efficiency vs m and k [15, 16, 18]

In SCALoM by combining an over-rated DC supply and pre-charged SC, the efficiency of RC charging loop is significantly enhanced as in Fig 6b according to the ratio, P. In SCALoM theory, a capacitor is never allowed to fully discharge during a cycle and low switching frequencies achieved to switch between charging and discharging phases. This can also eliminate the EMI and RFI filters in the circuit leading to the smaller number of components. Two successful applications of this technique are the supercapacitor-assisted LED (SCALED) [20, 21] and the supercapacitor-assisted low drop-out regulator (SCALDO) [22, 23].

B. Extending the SCALoM to SCA refrigerator

In this supercapacitor-assisted refrigerator (SCARef), we have used the SCALoM concept to reduce losses in the RC combination created by the resistive load (the refrigerator) and the SC module, during the charging phase of the converter. (SC module works as a loosless voltage dropper during charging time) This eliminates the need for a high-frequency DC-DC converter, the associated maximum power point tracking (MPPT) system, and a battery pack. If the DC equivalent resistance of the modified refrigerator is significantly higher than the parasitic resistance in the loop in Fig. 6a, losses associated with the r_p is consumed usefully by the refrigerator.

In the proposed design concept, a modified DC-operable inverter-driven refrigerator which was tested to operate from a wider DC voltage range from 255 to 325 V is connected to the solar panel in series with the SC bank as in Fig. 7a.

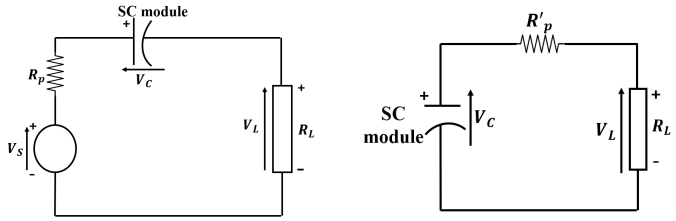

(a) (b)

Fig. 7: Concept of SCARef (a) Charging phase; (b) discharging phase

The SC module is designed for a nominal voltage of 300 V which will keep charging towards 320 V while the refrigerator will operate normally from 300 to 280 V. The moment the capacitor bank reaches the 320 V DC value, configuration switches to the parallel operation mode as depicted in Fig. 7b where the solar panel is free to charge another SC bank if necessary. In this operation, Fig 7a is equivalent to Fig 6a where R_L represents the refrigerator load. The constant current region of the solar PV system permits the SC bank to charge initially to 300 V by directly connecting to it. When the solar PV system powers the refrigerator while charging the SC bank, the variable voltage region of the solar PV system is used.

This discussion assumes the nominal solar array voltage of 600 V DC. The proposed system is allowed to work the range of input voltage from 580 to 620 V. For cases of lower values of DC source, the rated voltage of supercapacitor modules configuration could be easily modified. This research is in progress.

IV. A SCALED-DOWN SYSTEM FOR PROOF OF CONCEPT

A. SCA Converter for Camping Refrigerator

We tested the workability of SCA converter using a small camping refrigerator (BC 50, Sunrise) which is operable from 12/24 V DC supply. It was tested that the DC refrigerator is working from 23 V to 35 V under an operation region of 24 V. In this case, we used a laboratory power supply as input source, V_S in Fig. 6a, and a supercapacitor module of 33 V, 69 F. Initially SC bank was charged to 24V and increased the DC power supply by a multiplication factor of $m = 2$ according to the SCALoM concept to keep all elements in the loop to operate their nominal voltages.

The circuit was designed to operate in the following voltage ranges.

1) Operational voltage range of DC refrigerator: 24 V $\leq V_L \leq$ 32 V
2) Operational voltage range of SC bank: 24 V $\leq V_C \leq$ 32 V
3) Input voltage range: $58V \geq V_S \geq 55V$

During the charging phase of the SC, DC power supply powers the DC refrigerator. In this stage SC module voltage increases from 24 to 32 V while decreasing the DC

refrigerator voltage from 32 to 24 V at 56 V of DC supply voltage. When the DC refrigerator voltage comes to the lower value of 24V , the configuration shifted to the SC discharging phase by disconnecting the input power supply from the system. Then, SC discharged up to 24 V by maintaining the same voltage across the refrigerator and continue. Fig. 8a depicts the implementation of switching circuit between the charging and discharging phases of the SC of the SCALoM controller based on the switching logic as in Table II. Lab set up is shown in Fig. 8b. Fig. 9 shows the voltage variation across the SC bank and the DC refrigerator demonstrating the SCARef technique based on SCALoM concept.

Switching period of the SCA converter is about 20 minutes and demonstrate the very low frequency switching operation. Hence, the SCA converter would not have any EMI and RFI issues.

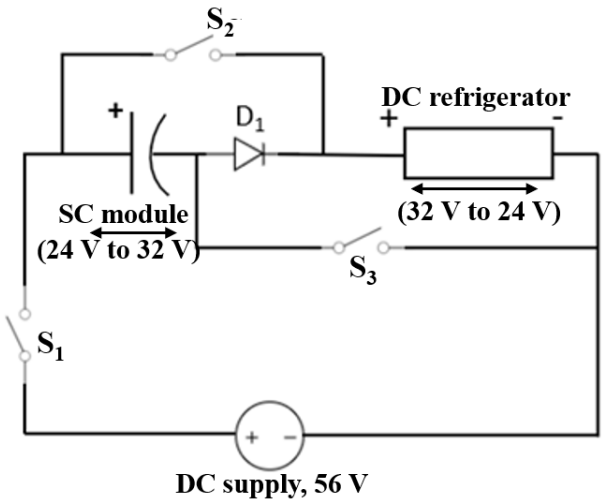

(a)

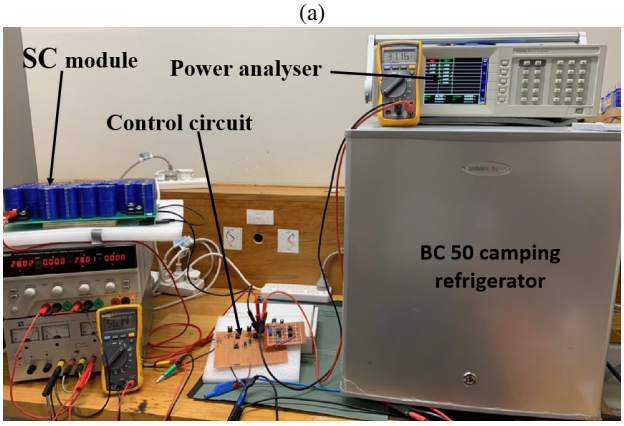

(b)

Fig. 8: Concept of SCA DC refrigerator (a) circuit arrangement of SCA DC refrigerator; (b) laboratory experimental setup

The efficiency of the SCA DC refrigerator during the capacitor charging phase can be evaluated from Fig. 6b by taking $m = 2$ and $k = 0.75$ according to the experimental setup for different values of P. P can be taken as 9 by considering R_L is much higher than the r_p in Fig. 6a with respect to parasitic resistance in the loop and the DC resistance in the refrigerator. Hence, efficiency was calculated to be 94.4% of the SCA DC refrigerator during the charging phase of the SC according to eq. 5. The measured efficiency of the overall SCA DC converter system for camping refrigerators for three different thermostat settings is indicated in Table III.

TABLE II: Switching arrangement of the SCA converter

Mode	S1	S2	S3
SC charging	ON	OFF	ON
SC discharging	OFF	ON	ON

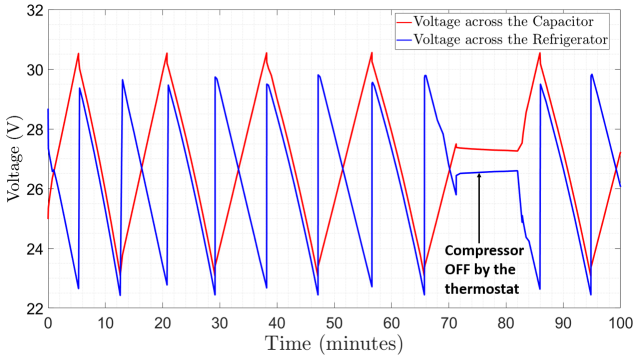

Fig. 9: Waveform of voltage variation between SC module and DC refrigerator

TABLE III: Efficiency measurements of SCA DC camping refrigerator

Thermostat settings	2	4	6
Energy efficiency (%)	93.3	93.5	93.6

For night operations, a DC home and its DC-powered white-ware can be operated by an efficient AC-DC converter derived from AC mains, if rechargeable batteries are to be eliminated. In the longer run supercapacitor device improvements will permit us to enhance the primary energy storage in a DC home by supercapacitor banks.

B. Loss contributors of SCA converter

To enhance the efficiency of the circuit, losses should be minimized when designing the circuit. The SC which has low ESR used as the energy storage device and the series lossless voltage dropper in the SCA converter increases the efficiency of the circuit by reusing the stored energy in the SC. Following are some of the secondary loss contributors to the circuit.

1) ESR and the leakage current losses in the SCs:
In this SCA converter, SC bank is charged and discharged with the current drawn by the refrigerator. I^2R ohmic loss can be presented in the circuit due to ESR present in the SC bank. Having a very low ESR, less than 50 mΩ range[24] , this loss can be minimized.

2) Switching losses:
Using MOSFET having low R_{DS} on resistance as the switches, conduction switching losses minimized and high frequency switching losses also eliminated having significant low switching frequency.

3) Control circuit energy consumption:
Simple Schmitt-trigger detection circuit is used to drive the MOSFET switches in the control circuit and it draws 50 mA of current. Therefore, power consumption by the control circuit was fairly small compared to a processor-based switching converter.

V. Conclusion and Future works

This paper presents how the recently published SCALoM theory can be used in a DC home environment in which a traditional AC-operable household refrigerator is modified to operate on a DC bus and an energy buffer on a supercapacitor module. Most important property of this new concept is the reduction of power consumption by around 5% in commercially available modified DC-operable inverter-driven refrigerator. This technique also helps to reduce the product cost by removing the AC-DC converters. In addition, the switching sequence is at an extra low frequency in the range of hertz to fractional hertz which reduces the EMI and RFI.

As our future work, we are currently developing the high voltage capable SC modules and the associated switching modules for the 230 V AC refrigerator described in this paper. One major target is to reduce the renewable DC rail voltage to use a SC module with lower voltage to keep the cost low.

Acknowledgement

The authors acknowledge the research funding provided by the Ministry of Business, Innovation, and Employment New Zealand through the Future Architecture Network (FAN) project of the Advanced Energy Technology Program (AETP) and the Fisher & Paykel Appliances Holdings Ltd for donating an inverter-driven refrigerator for the research.

References

[1] F. S. Al-Ismail, "DC microgrid planning, operation, and control: A comprehensive review," *IEEE Access*, vol. 9, pp. 36154–36172, 2021.

[2] R. Singh, G. F. Alapatt, and G. Bedi, "Why and how photovoltaics will provide cheapest electricity in the 21st century," *Facta Universitatis, Series: Electronics and Energetics*, vol. 27, no. 2, pp. 275–298, 2014.

[3] V. Vossos, K. Garbesi, and H. Shen, "Energy savings from direct-DC in US residential buildings," *Energy and Buildings*, vol. 68, pp. 223–231, 2014.

[4] U. Manandhar, A. Ukil, and T. K. K. Jonathan, "Efficiency comparison of DC and AC microgrid," in *2015 IEEE Innovative Smart Grid Technologies-Asia (ISGT ASIA)*, pp. 1–6, IEEE, 2015.

[5] B. Glasgo, I. L. Azevedo, and C. Hendrickson, "How much electricity can we save by using direct current circuits in homes? Understanding the potential for electricity savings and assessing feasibility of a transition towards DC powered buildings," *Applied Energy*, vol. 180, pp. 66–75, 2016.

[6] M. A. Rodriguez-Otero and E. O'Neill-Carrillo, "Efficient home appliances for a future DC residence," in *2008 IEEE Energy 2030 Conference*, pp. 1–6, IEEE, 2008.

[7] G. Makarabbi, V. Gavade, R. Panguloori, and P. Mishra, "Compatibility and performance study of home appliances in a DC home distribution system," in *2014 IEEE International Conference on Power Electronics, Drives and Energy Systems (PEDES)*, pp. 1–6, 2014.

[8] U. Boeke and M. Wendt, "Dc power grids for buildings," in *2015 IEEE First International Conference on DC Microgrids (ICDCM)*, pp. 210–214, IEEE, 2015.

[9] T. Qureshi and S. Tassou, "Variable-speed capacity control in refrigeration systems," *Applied thermal engineering*, vol. 16, no. 2, pp. 103–113, 1996.

[10] C. Rasmussen and E. Ritchie, "Variable speed brushless DC motor drive for household refrigerator compressor," in *1997 Eighth International Conference on Electrical Machines and Drives (Conf. Publ. No. 444)*, pp. 128–132, 1997.

[11] D. M. Ionel, "High-efficiency variable-speed electric motor drive technologies for energy savings in the US residential sector," in *2010 12th International Conference on Optimization of Electrical and Electronic Equipment*, pp. 1403–1414, IEEE, 2010.

[12] W. R. Chang, D. Y. Liu, S. G. Chen, N. Y. Wu, *et al.*, "The components and control methods for implementation of inverter-controlled refrigerators/freezers," 2004.

[13] T. R. DuMoulin and D. A. Collings, "Higher efficiencies by means of variable-speed technology in a domestic refrigeration application," *ASHRAE Transactions*, vol. 104, p. 652, 1998.

[14] Fisher and Paykel, *ActiveSmart Refrigerator*, version 4, 5 and 6 models ed., 2022.

[15] N. Kularatna, K. Subasinghage, K. Gunawardane, D. Jayananda, and T. Ariyarathna, "Supercapacitor-assisted techniques and supercapacitor-assisted loss management concept: New design approaches to change the roadmap of power conversion systems," *Electronics*, vol. 10, no. 14, p. 1697, 2021.

[16] N. Kularatna and D. Jayananda, "Supercapacitor-based long time-constant circuits: A unique design opportunity for new power electronic circuit topologies," *IEEE Industrial Electronics Magazine*, vol. 14, no. 2, pp. 40–56, 2020.

[17] N. Kularatna, K. Milani, and W. H. Round, "Supercapacitor energy storage in solar application: A design approach to minimize a fundamental loss issue by partitioning the load and the storage device," in *2015 IEEE 24th International Symposium on Industrial Electronics (ISIE)*, pp. 1308–1312, 2015.

[18] N. Kularatna and K. Gunawardane, *Energy Storage Devices for Renewable Energy-Based Systems: Rechargeable Batteries and Supercapacitors*. Academic Press, 2021.

[19] N. Kularatna, "Supercapacitors improve the performance of linear power-management circuits: Unique new design options when capacitance jump from micro-farads to farads with a low equivalent series resistance," *IEEE Power Electronics Magazine*, vol. 3, no. 1, pp. 45–59, 2016.

[20] D. Jayananda, N. Kularatna, and D. A. Steyn-Ross, "Supercapacitor-assisted LED (SCALED) technique for renewable energy systems: a very low frequency design approach with short-term DC-UPS capability eliminating battery banks," *IET Renewable Power Generation*, vol. 14, no. 9, pp. 1559–1570, 2020.

[21] D. Jayannada, N. Kularatna, and D. A. Steyn-Ross, "Supercapacitor assisted LED lighting (SCALED) for DC-micro grids," in *2019 IEEE Third International Conference on DC Microgrids (ICDCM)*, pp. 1–6, IEEE, 2019.

[22] K. Gunawardane and N. Kularatna, "Supercapacitor-assisted low dropout regulator technique: a new design approach to achieve high-efficiency linear DC–DC converters," *IET Power Electronics*, vol. 11, no. 2, pp. 229–238, 2018.

[23] K. Kankanmage and N. Kulatana, "Supercapacitor assisted LDO (SCALDO) technique an extra low frequency design approach to high efficiency DC-DC converters and how it compares with the classical switched capacitor converters," in *2013 Twenty-Eighth Annual IEEE Applied Power Electronics Conference and Exposition (APEC)*, pp. 1979–1984, IEEE, 2013.

[24] SAMWHA Electric Co.,Ltd., *Green-Cap(Electrical Double Layer Capacitors)*, 08 2023.